IMPACT OF LIDAR SYSTEM CALIBRATION ON THE RELATIVE AND ABSOLUTE ACCURACY OF THE ADJUSTED POINT CLOUD

A. Habib [a] *, A. Kersting [a], K. Bang[a]

[a] Department of Geomatics Engineering, University of Calgary, Canada, (ahabib, ana.kersting, kibang)@ucalgary.ca

Commission I, WG I/5 and WGI/3

KEY WORDS: LIDAR, Calibration, Impact Analysis, Adjustment, Error, Laser scanning

ABSTRACT:

The availability of 3D surface data is valuable for several industrial, public, and military applications. Light Detection And Ranging (LiDAR) is an active sensor system capable of collecting 3D information from an object surface using directly geo-referenced laser pulses. Accurate and dense LiDAR data can be utilized for photogrammetric data geo-referencing and segmentation of 3D buildings. LiDAR data contaminated by systematic errors (e.g., biases in the mounting parameters) cannot guarantee the achievement of the expected accuracy and discrepancies might occur between overlapping strips. This paper introduces an alternative method for LiDAR system calibration. In the proposed method, biases in LiDAR system parameters are estimated using time-tagged point cloud and trajectory data (position only). Unlike conventional calibration methods, the proposed method does not require raw measurements such as GPS/INS observations, mirror scan angles, and ranges for the laser footprints. Biases in the system mounting parameters are estimated while reducing discrepancies between conjugate surface elements in overlapping strips. Estimated biases are then used to adjust the point cloud. The influence of LiDAR system calibration is analyzed through the evaluation of the relative and absolute accuracy before/after the calibration. The evaluation of the relative accuracy will be based on quantifying the degree of compatibility between conjugate surface elements in overlapping strips before and after the calibration procedure. In addition, the impact of the LiDAR system calibration on the absolute accuracy of the point cloud is evaluated by using the LiDAR data for photogrammetric georeferencing before and after performing the proposed calibration procedure. The outcome of the photogrammetric reconstruction will be evaluated through check point analysis. The experimental results have shown that the proposed calibration procedure improves the relative and absolute accuracy of the LiDAR point cloud.

1. INTRODUCTION

A LiDAR system is composed of a laser ranging and scanning unit and a position and orientation system (POS), which consists of an integrated differential global positioning system (DGPS) and an inertial measurement unit (IMU). The laser scanner measures distances from the sensor to the ground. The integrated GPS/IMU observations provide the position and attitude information of the scanner. The coordinates of the LiDAR points are the result of combining the derived measurements from each of its system components, as well as the mounting parameters relating such components. The relationship between the system measurements and parameters is embodied in the LiDAR equation (Vaughn et al., 1996; Schenk, 2001; El-Sheimy et al., 2005), Equation 1. As it can be seen in Figure 1, the position of the laser point, $\vec{X}_G$, can be derived through the summation of three vectors ($\vec{X}_o$, $\vec{P}_G$ and $\vec{\rho}$) after applying the appropriate rotations: $R_{yaw,\ pitch,\ roll}$, $R_{\Delta\omega,\Delta\phi,\Delta\kappa}$ and $R_{\alpha,\ \beta}$. In this equation, $\vec{X}_o$ is the vector from the origin of the ground reference frame to the origin of the IMU coordinate system, $\vec{P}_G$ is the offset between the laser unit and IMU coordinate systems (lever-arm offset vector), and $\vec{\rho}$ is the laser range vector whose magnitude is equivalent to the distance from the laser firing point to its footprint. It should be noted that $\vec{X}_o$ is derived through the GPS/INS integration process while considering the lever-arm offset vector between the IMU body frame and the phase centre of the GPS antenna. The term $R_{yaw,\ pitch,\ roll}$ stands for the rotation matrix relating the ground and IMU coordinate systems – which is derived through the GPS/INS integration process, $R_{\Delta\omega,\Delta\phi,\Delta\kappa}$ represents the rotation matrix relating the IMU and laser unit coordinate systems – which is defined by the bore-sighting angles, and $R_{\alpha,\ \beta}$ refers to the rotation matrix relating the laser unit and laser beam coordinate systems with α and β being the mirror scan angles. For a linear scanner, which is the focus of this research work, the mirror is rotated in one direction only leading to zero α angle. The involved quantities in the LiDAR equation are all measured during the acquisition process except for the bore-sighting angles and lever-arm offset vector (mounting parameters), which are usually determined through a calibration procedure.

The quality of the derived point cloud from a LiDAR system depends on inherent random and systematic errors in the system measurements and parameters. Random errors, regardless of their magnitude, will not lead to systematic discrepancies between conjugate surface elements in overlapping strips. Systematic errors, on the other hand, will result in inconsistencies among neighbouring strips, and are mainly caused by biases in the mounting parameters relating the system components as well as biases in the system measurements. A detailed description of LiDAR errors can be found in Huising and Pereira (1998), Baltsavias (1999), Schenk (2001), and Glennie (2007).

* Corresponding author.

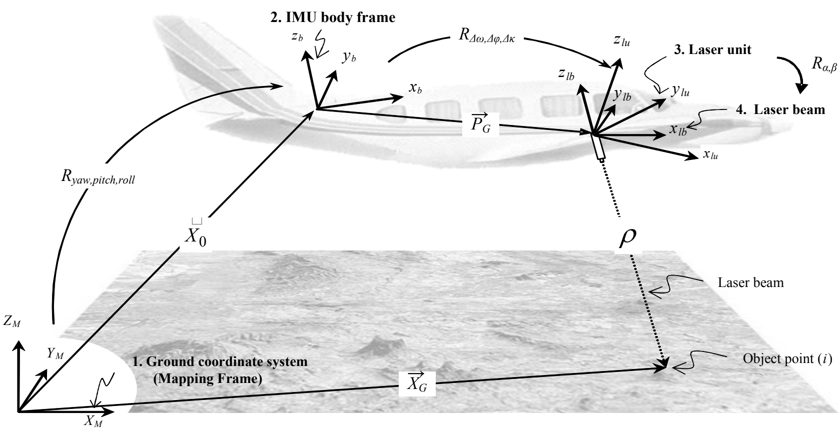

Figure 1. Coordinate systems and involved quantities in the LiDAR equation

$$\vec{X}_G = \vec{X}_o + R_{yaw,\ pitch,\ roll}\ \vec{P}_G + R_{yaw,\ pitch,\ roll}\ R_{\Delta\omega,\ \Delta\varphi,\ \Delta\kappa}\ R_{\alpha,\ \beta}\begin{bmatrix}0\\0\\-\rho\end{bmatrix} \quad (1)$$

The elimination and/or reduction of the effect of systematic errors in the system parameters have been the focus of LiDAR research in the past few years. The existing approaches can be classified into two main categories: system driven (calibration) and data driven (strip adjustment) methods. System driven (or calibration) methods, which are considered by many researchers as the ideal solution (e.g., Filin, 2001; Morin, 2002; Skaloud and Lichti, 2006; Friess, 2006), are based on the physical sensor model relating the system measurements/parameters to the ground coordinates of the LiDAR points. These methods require the original observations (GPS/INS positions and attitudes, and the laser measurements) or at least the trajectory and time-tagged point cloud (Burman, 2000; Toth, 2002), which might not be directly available to the end-user. Due to that fact, several approaches relying solely on the LiDAR point cloud coordinates, categorized as data-driven methods (or strip adjustment methods), have been proposed by several authors (Kilian et al., 1996; Crombaghs et al., 2000; Maas, 2002; Bretar et al., 2004; Filin and Vosselman, 2004; Pfeifer et al., 2005; Kager, 2004). In this approach, the effects of systematic errors are usually modeled by straightforward transformation function between the laser strip coordinate system and a reference coordinate system.

The objective of this paper is to introduce a new calibration procedure that overcomes the limitation of existing calibration procedures in terms of requirement for raw observations and control information. Moreover, the proposed calibration procedure is based on common primitives that can be identified in LiDAR data over urban and rural areas. This calibration procedure – denoted as "Quasi-Rigorous Method" – requires time-tagged LiDAR point cloud and navigation data (trajectory position) only. The paper starts by investigating the mathematical model relating conjugate surface elements in overlapping strips in the presence of systematic errors in the system mounting parameters. The mathematical derivation is based on a simplified LiDAR equation, which is established with the help of few reasonable assumptions. The performance and impact of the proposed calibration procedure on the relative and absolute accuracy of the LiDAR point cloud is evaluated through experimental results from real data. Finally, the paper presents some conclusions and recommendations for future work.

2. PROPOSED CALIBRATION PROCEDURE

In this section, the proposed calibration procedure, which makes use of time-tagged point cloud and trajectory position data, is presented. The introduced method utilizes LiDAR data in overlapping strips, where biases in the system mounting parameters are estimated while reducing discrepancies between conjugate surface elements in overlapping strips.

The proposed method is denoted as "Quasi-rigorous" in view of the fact that few reasonable assumptions are undertaken in the utilized mathematical model. The considered assumptions in the mathematical derivation are as follows: a) we are dealing with a linear scanner, b) the LiDAR system is almost vertical (i.e., pitch and roll angles are almost zero and can be ignored), and c) the LiDAR system has relatively small bore-sighting angles. In other words, this method only assumes that we are dealing with a linear scanner and that the LiDAR system unit is almost vertical, which is quite realistic for flight missions using a fixed wing platform. Such assumptions simplify the LiDAR geometric model as represented by Equation 1 to the form in Equation 2.

$$\vec{X}_G = \vec{X}_o + \begin{bmatrix}\cos\kappa & -\sin\kappa & 0\\ \sin\kappa & \cos\kappa & 0\\ 0 & 0 & 1\end{bmatrix}\begin{bmatrix}\Delta X\\ \Delta Y\\ \Delta Z\end{bmatrix} + \begin{bmatrix}\cos\kappa & -\sin\kappa & 0\\ \sin\kappa & \cos\kappa & 0\\ 0 & 0 & 1\end{bmatrix}\begin{bmatrix}1 & -\Delta\kappa & \Delta\varphi\\ \Delta\kappa & 1 & -\Delta\omega\\ -\Delta\varphi & \Delta\omega & 1\end{bmatrix}\begin{bmatrix}x\\ 0\\ z\end{bmatrix} \quad (2)$$

- $\Delta X, \Delta Y, \Delta Z$ are the components of the lever-arm offset vector $\vec{P}_G$,
- z is the vertical coordinate of the laser point with respect to the laser unit coordinate system, and
- x is the lateral coordinate of the laser point with respect to the laser unit coordinate system, which is the lateral distance (with the appropriate sign) between the LiDAR point in question and the projection of the flight trajectory onto the ground.

The LiDAR point coordinates $\vec{X}_G$, as presented in Equation 2, is function of the system mounting parameters $\vec{x}$ and measurements $\vec{l}$ (Equation 3), and represent the true point coordinates $\vec{X}_{True}$. In the presence of biases in the system mounting parameters, the LiDAR point coordinates will become biased ($\vec{X}_{Biased}$) and will be function of the system parameters and measurements as well as biases in the system parameters ($\delta\vec{x}$), as expressed by Equation 4. In this paper, we will investigate the impact of biases in mounting parameters, i.e., biases in the lever-arm offset components ($\delta\Delta X, \delta\Delta Y, \delta\Delta Z$) and biases in the bore-sighting angles ($\delta\Delta\omega, \delta\Delta\varphi, \delta\Delta\kappa$) (Equation 4). Equation 4 can be linearized with respect to the system parameters using Taylor series expansion, producing the form in Equations 5 and 6, after ignoring second and higher order terms. The term $\frac{\partial f}{\partial \vec{x}}$ represents the partial derivatives with respect to the system parameters, while the term $\frac{\partial f}{\partial \vec{x}}\delta\vec{x}$ represents the impact of the system biases onto the derived point cloud coordinates ($\delta\vec{X}_G$).

$$\vec{X}_G = \vec{X}_{True} = f(\vec{x}, \vec{l}) \tag{3}$$

where,

$$\vec{x} = (\Delta X, \Delta Y, \Delta Z, \Delta\omega, \Delta\varphi, \Delta\kappa)$$

$$\vec{l} = \left(\vec{X}_o, \omega, \varphi, \kappa, \beta, \rho\right)$$

$$\vec{X}_{Biased} = f(\vec{x} + \delta\vec{x}, \vec{l}) \tag{4}$$

where,

$$\delta\vec{x} = (\delta\Delta X, \delta\Delta Y, \delta\Delta Z, \delta\Delta\omega, \delta\Delta\varphi, \delta\Delta\kappa)$$

$$\vec{X}_{Biased} \approx f(\vec{x}, \vec{l}) + \frac{\partial f}{\partial \vec{x}}\delta\vec{x} = \vec{X}_{True} + \begin{bmatrix} \delta X_G \\ \delta Y_G \\ \delta Z_G \end{bmatrix} \tag{5}$$

$$\vec{X}_{Biased} \approx \vec{X}_{True} + \begin{bmatrix} \delta X_G \\ \delta Y_G \\ \delta Z_G \end{bmatrix}_{\delta\Delta X,\, \delta\Delta Y,\, \delta\Delta Z} + \begin{bmatrix} \delta X_G \\ \delta Y_G \\ \delta Z_G \end{bmatrix}_{\delta\Delta\omega,\, \delta\Delta\varphi,\, \delta\Delta\kappa} \tag{6}$$

The mathematical relationship between conjugate points in overlapping strips can be derived by rewriting Equation 6 for two overlapping strips (*A* and *B*) and subtracting the resulting equations from each other. Such a relationship is shown in Equation 7. This equation is the final linear observation equation, which allows us to recover the biases in the system mounting parameters $(\delta\Delta X, \delta\Delta Y, \delta\Delta Z, \delta\Delta\omega, \delta\Delta\phi, \delta\Delta\kappa)$. It should be noted that, when using only overlapping strips, the vertical bias in the lever-arm offset components ($\delta\Delta Z$) cannot be estimated. Such inability is caused by the fact that a vertical bias in the lever-arm offset components produces the same effect regardless of the flying direction, flying height, or scan angle.

A detailed analysis of the impact of biases in the system parameters on the derived LiDAR point cloud in terms of flying direction, flying height, and scan angle dependency is presented in Habib et al., 2009. In this work, the flight configuration that maximizes the impact and decouples systematic errors in the mounting parameters is investigated. It was mathematically demonstrated that working with four strips which are captured from two flying heights in opposite directions with 100% overlap are optimal for the recovery of the planimetric lever-arm offset parameters as well as the bore-sighting pitch and roll biases. In addition, two flight lines, which are flown in the same direction with the least overlap possible, are optimal for the recovery of biases in the bore-sighting yaw and roll angles.

Once the biases are recovered, we can reconstruct the corrected point cloud using Equation 8. In this equation, the terms $(\delta\hat{\Delta}X, \delta\hat{\Delta}Y, \delta\hat{\Delta}\omega, \delta\hat{\Delta}\phi, \delta\hat{\Delta}\kappa)$ define the estimated biases in the mounting parameters.

$$\begin{bmatrix} X_A \\ Y_A \\ Z_A \end{bmatrix}_{Biased} - \begin{bmatrix} X_B \\ Y_B \\ Z_B \end{bmatrix}_{Biased} = \begin{bmatrix} (\cos\kappa_A - \cos\kappa_B)\delta\Delta X - (\sin\kappa_A - \sin\kappa_B)\delta\Delta Y \\ (\sin\kappa_A - \sin\kappa_B)\delta\Delta X + (\cos\kappa_A - \cos\kappa_B)\delta\Delta Y \\ 0 \end{bmatrix} + \begin{bmatrix} (\sin\kappa_A z_A - \sin\kappa_B z_B)\delta\Delta\omega \\ -(\cos\kappa_A z_A - \cos\kappa_B z_B)\delta\Delta\omega \\ 0 \end{bmatrix} + \begin{bmatrix} (\cos\kappa_A z_A - \cos\kappa_B z_B)\delta\Delta\phi \\ (\sin\kappa_A z_A - \sin\kappa_B z_B)\delta\Delta\phi \\ -(x_A - x_B)\delta\Delta\phi \end{bmatrix} + \begin{bmatrix} -(\sin\kappa_A x_A - \sin\kappa_B x_B)\delta\Delta\kappa \\ (\cos\kappa_A x_A - \cos\kappa_B x_B)\delta\Delta\kappa \\ 0 \end{bmatrix} + \tag{7}$$

$$\begin{bmatrix} X \\ Y \\ Z \end{bmatrix}_{Corrected} = \begin{bmatrix} X \\ Y \\ Z \end{bmatrix}_{Biased} - \begin{bmatrix} \cos\kappa\delta\hat{\Delta}X - \sin\kappa\delta\hat{\Delta}Y + \sin\kappa z\delta\hat{\Delta}\omega + \cos\kappa z\delta\hat{\Delta}\phi + \sin\kappa x\delta\hat{\Delta}\kappa \\ \sin\kappa\delta\hat{\Delta}X + \cos\kappa\delta\hat{\Delta}Y - \cos\kappa z\delta\hat{\Delta}\omega + \sin\kappa z\delta\hat{\Delta}\phi - \cos\kappa x\delta\hat{\Delta}\kappa \\ -x\delta\hat{\Delta}\phi \end{bmatrix} \tag{8}$$

The procedure for estimating the necessary quantities $(x, z, \text{and } k)$ presented in Equation 7 using the available data (time-tagged point cloud and trajectory positions), is as follows:

I. For a LiDAR point mapped at time (*t*), we search in the trajectory file for positions within a certain time interval ($t - \Delta t$, $t + \Delta t$);
II. Then, a straight line is fitted through the selected trajectory positions to come up with a local estimate of the trajectory, as shown in Figure 2. After defining the local trajectory, the necessary quantities can be estimated as follows:
   - *x,* which is the lateral coordinate of the laser point with respect to the laser unit coordinate system, can be determined by computing the normal distance (with the appropriate sign) between the LiDAR point and the interpolated trajectory data (Figure 2). The intersection of the normal from the LiDAR point to the interpolated trajectory will define the position of the trajectory at time *t*;
   - *z,* which is the vertical coordinate of the laser point with respect to the laser unit coordinate system, can be determine by subtracting the elevation of the laser

firing point (H) at time t, given by the interpolated flight trajectory, from the LiDAR point elevation (Z), i.e., $z = Z - H$; and

- κ, which is the trajectory heading, can be computed once we have the local estimate of the trajectory and its direction (defined by the neighbouring trajectory positions);

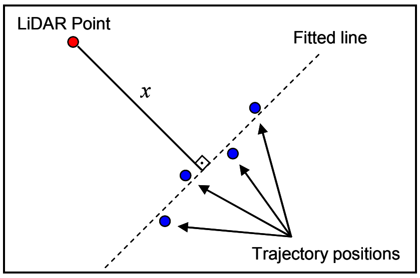

Figure 2. Lateral distance between the LiDAR point in question and the projection of the flight trajectory onto the ground

One should note that the established mathematical model for the calibration procedure is derived based on point primitives (i.e., conjugate points in overlapping strips). However, point-to-point correspondence in overlapping strips cannot be assumed due to the irregular nature of the LiDAR points. In this research, conjugate point and TIN patch pairs are used as primitives and the Iterative Closest Patch (ICPatch) procedure is applied to establish their correspondence. For more information regarding the ICPatch method, interested readers can refer to Habib et al., 2009a and Habib et al., 2010. The utilization of conjugate point-patch pairs for the estimation of biases in the system parameters is accomplished through a weight modification for one of the points defining the TIN vertices (Habib et al., 2009b).

3. EVALUATION OF THE IMPACT OF THE CALIBRATION PROCEDURE

In this work, the impact of the proposed LiDAR system calibration procedure is analyzed through the evaluation of the relative and absolute accuracy of the LiDAR data before and after the calibration.

The impact on the relative accuracy will be assessed by quantifying the degree of compatibility between conjugate surface elements in overlapping strips before and after reconstructing the point cloud using the estimated system biases (Equation 8). The compatibility will be evaluated qualitatively and quantitatively. The qualitative evaluation will be performed by visual inspection of profiles generated using the original and adjusted point clouds to check any improvements in the quality of fit between overlapping strips. The quantitative assessment, on the other hand, will be performed by computing the 3D transformation parameters (discrepancies) between the overlapping strips before and after the calibration procedure. For the computation of the 3D transformation parameters, the ICPatch method will be employed. The implementation details of this method can be found in Habib et al., 2009a and Habib et al., 2010.

To evaluate the impact of the calibration procedure on the absolute accuracy of the point cloud, LiDAR linear features will be used for the geo-referencing of an image block covering the same area. The methodology used for photogrammetric geo-referencing utilizing control linear features is detailed in Shin et al., 2007. The absolute accuracy of the derived ground coordinates from the geo-referenced image block is evaluated using a check point analysis.

4. EXPERIMENTAL RESULTS

4.1 Dataset Description

To evaluate the performance and test the validity of the proposed calibration methodology, a LiDAR dataset captured by a Leica ALS50, which complies with the optimum flight configuration, was utilized. The optimum flight configuration, as discussed in section 2, consists of four strips which are captured from two flying heights in opposite directions with as much overlap as possible, and two flight lines, which are flown in the same direction with the least overlap possible. This configuration allows for the maximization of the impact of systematic biases and has the ability to decouple the different biases from each other. Figure 3 shows the characteristics of the acquired dataset and Table 1 presents the utilized overlapping strip pairs.

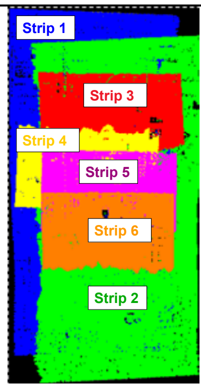

Strip Number	Flying Height	Direction
1	1150 m	N-S
2	1150 m	S-N
3	539 m	E-W
4	539 m	W-E
5	539 m	E-W
6	539 m	E-W

Figure 3. Dataset Configuration

Table 1. Overlapping strip pairs used in the calibration procedure

Overlapping Strips Cases	% of Overlap	Direction
Strips 1&2	80%	Opposite directions
Strips 3&4	25%	Opposite directions
Strips 4&5	75%	Opposite directions
Strips 5&6	50%	Same direction

4.2 Calibration Results

The estimated biases in the system mounting parameters from the proposed calibration procedure are presented in Table 2. Note that all mounting parameters biases are reported except the vertical bias in the lever-arm offset components $\delta\Delta Z$. As already mentioned, this bias cannot be estimated using overlapping strips due to the fact that it produces the same effect regardless of the flying direction, flying height, or scan angle. It can be noted in Table 2 that a significant bias in the bore-sighting roll angle was detected.

Table 2. Estimated biases in the mounting parameters

$\delta\Delta X$ (m)	$\delta\Delta Y$ (m)	$\delta\Delta\omega$ (")	$\delta\Delta\phi$ (")	$\delta\Delta\kappa$ (")
-0.01	0.02	-40.2	-90.9	-4.58

4.3 Impact Analysis

The impact of the calibration procedure on the relative accuracy of the point cloud is evaluated qualitatively and quantitatively. The qualitative evaluation is performed by visual inspection of profiles generated using the original and adjusted point cloud to check any improvements in the quality of fit between overlapping strips. The improvement in the strips compatibility is illustrated in Figure 4, which shows a profile involving strips 1, 2, and 3 along the *X* direction, before and after the calibration procedure. The quantitative assessment, on the other hand, is performed by computing the discrepancies before and after the calibration procedure. The computed discrepancies are reported in Table 3. In this table, a significant improvement can be observed, especially in the across flight direction between strips flown in opposite directions (X_T direction for strips 1&2, and Y_T direction for strips 3&4 and strips 4&5). This is expected since a larger bias was estimated in the bore-sight roll angle, which mainly affects the across-flight direction.

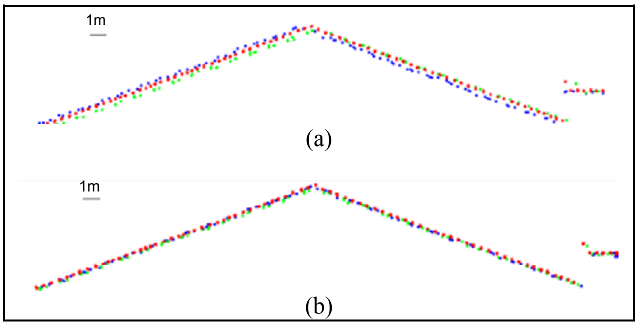

Figure 4. Profiles before and after the calibration procedure

Table 3. Discrepancies between overlapping strips after applying the calibration parameters

Before Calibration			After Calibration		
Strips 1&2			Strips 1&2		
X_T (m)	Y_T (m)	Z_T(m)	X_T(m)	Y_T(m)	Z_T(m)
1.10	-0.32	-0.01	0.11	0.07	-0.05
ω(deg)	ϕ(deg)	κ(deg)	ω(deg)	ϕ(deg)	κ(deg)
0.0001	-0.052	-0.002	0.0012	-0.0016	-0.0051
Strips 3&4			Strips 3&4		
X_T (m)	Y_T (m)	Z_T(m)	X_T(m)	Y_T(m)	Z_T(m)
0.18	0.41	-0.01	-0.01	-0.01	0.01
ω(deg)	ϕ(deg)	κ(deg)	ω(deg)	ϕ(deg)	κ(deg)
0.0484	-0.0005	-0.0011	0.0052	0.0008	-0.0045
Strips 4&5			Strips 4&5		
X_T (m)	Y_T (m)	Z_T(m)	X_T(m)	Y_T(m)	Z_T (m)
-0.13	-0.58	-0.12	0.07	-0.04	0.03
ω(deg)	ϕ(deg)	κ(deg)	ω(deg)	ϕ(deg)	κ(deg)
-0.0506	-0.0004	-0.0055	0.0039	-0.0001	-0.0054
Strips 5&6			Strips 5&6		
X_T (m)	Y_T (m)	Z_T (m)	X_T (m)	Y_T (m)	Z_T (m)
-0.06	-0.09	-0.08	-0.05	-0.03	0.03
ω(deg)	ϕ(deg)	κ(deg)	ω(deg)	ϕ(deg)	κ(deg)
-0.0049	0.0014	0.0068	0.0005	0.0018	0.0076

To check the impact of the calibration procedure on the absolute accuracy, LiDAR linear features have been extracted and used for the geo-referencing of an image block, which has been captured by a Rollei P-65 digital camera over the same area from two different flying heights (~550 and ~1200 m). The utilized camera has an array dimension of 8984x6732 pixels and a focal length of 60 mm.The quality of the derived ground coordinates from the geo-referenced image block was evaluated using a check point analysis. The results from the RMSE analysis for a total of 37 check points (GPS surveyed points) using the derived control linear features from the LiDAR point cloud before and after the calibration procedure are listed in Table 4. Significant improvement in the planimetric accuracy can be observed. As expected, almost no improvement in the vertical accuracy is observed since detected biases in the system mounting parameters mainly affect the horizontal accuracy.

Table 4. RMSE analysis of the photogrammetric check points using extracted control linear features from the LiDAR data before and after the calibration procedure

	Before Calibration	*After Calibration*
Mean ΔX (m)	-0.03	-0.01
Mean ΔY (m)	-0.18	-0.05
Mean ΔZ (m)	0.15	0.11
σ_X (m)	0.11	0.05
σ_Y (m)	0.15	0.06
σ_Z (m)	0.17	0.18
$RMSE_X$ (m)	0.11	0.05
$RMSE_Y$ (m)	0.23	0.07
$RMSE_Z$ (m)	0.23	0.21
$RMSE_{TOTAL}$ (m)	0.34	0.23

5. CONCLUSIONS AND RECOMMENDATIONS FOR FUTURE WORK

In this paper, a new calibration procedure for the estimation of biases in the system mounting parameters was introduced. The proposed method, denoted as "Quasi-rigorous", is based on the following assumptions: a) we are dealing with a linear scanner, b) the LiDAR system is almost vertical (i.e., pitch and roll angles are almost zero), and c) the LiDAR system has relatively small bore-sighting angles. This method can deal with non-parallel strips and can handle heading variations and varying elevation heights since it makes use of time-tagged point cloud and trajectory position data.

The performance of the developed calibration procedure has been verified using a real dataset. It was shown that collected LiDAR data might exhibit significant incompatibilities due to insufficient calibration procedures. The impact of the calibration method on the relative and absolute accuracy has been verified. The impact on the relative accuracy has been evaluated qualitatively and quantitatively. The qualitative evaluation of the calibration procedure was performed by visual inspection of profiles generated using the original and adjusted point cloud to check any improvements in the quality of fit between overlapping strips. The quantitative evaluation, on the other hand, was performed by estimating the discrepancies between overlapping strips before and after reconstructing the LiDAR point cloud using the estimated biases in the system parameters. Qualitative and quantitative assessments have demonstrated a significant improvement in the quality of fit between overlapping strips – visually checked in profiles and in the computed discrepancies (e.g., the discrepancy between strips 1&2 across the flight direction was reduced from 1.10m to few centimetres). The impact on the absolute accuracy was assessed by using the LiDAR data for photogrammetric georeferencing before and after performing the proposed calibration procedure. The outcome of the photogrammetric reconstruction was evaluated through check point analysis. Significant improvement in the horizontal accuracy was

demonstrated after removing the effect of estimated biases in the system parameters.
Future work will focus on extending the mathematical model to include biases in the range as well as mirror angle measurements. In addition, the incorporation of control information in the calibration method will be investigated. Moreover, more testing with real data from operational systems will be performed.

ACKNOWLEDGEMENT

This work was supported by the Canadian GEOIDE NCE Network (SII-72) and the National Science and Engineering Council of Canada (Discovery Grant). The authors would like to thank McElhanney Consulting Services Ltd, BC, Canada for providing the real LiDAR and image datasets. Also, the authors are indebted to Mr. Dan Tresa, McElhanney Consulting Services Ltd, for the valuable feedback.

REFERENCES

Baltsavias, E., 1999. Airborne laser scanning: existing systems and firms and other resources. *ISPRS Journal of Photogrammetry and Remote Sensing*, 54 (2-3), pp. 164-198.

Bretar F., M. Pierrot-Deseilligny, and M. Roux, 2004. Solving the Strip Adjustment Problem of 3D Airborne Lidar Data. *Proceedings of the IEEE IGARSS'04,* 20-24 September, Anchorage, Alaska, 7, pp. 4734-4737.

Burman, H., 2000. *Calibration and Orientation of Airborne Image and Laser Scanner Data Using GPS and INS*. Ph.D. dissertation, Royal Institute of Technology, Stockholm. 125pages.

Crombaghs, M., E. De Min, and R. Bruegelmann, 2000. On the Adjustment of Overlapping Strips of Laser Altimeter Height Data. *International Archives of Photogrammetry and Remote Sensing*, 33(B3/1), pp. 230-237.

El-Sheimy, N., C. Valeo, and A. Habib, 2005. *Digital Terrain Modeling: Acquisition, Manipulation And Applications*. Artech House Remote Sensing Library. 257 pages.

Friess, P., 2006. Toward a rigorous methodology for airborne laser mapping. *Proceedings EuroCOW*. 25-27 January, Castelldefels, Spain. 7 pages (on CD-ROM).

Filin, S., 2001. *Calibration of spaceborne and airborne laser altimeters using natural surfaces*. PhD Dissertation. Department of Civil and Environmental Engineering and Geodetic Science, the Ohio-State University, Columbus, OH. 129 pages.

Filin, S. and G. Vosselman, 2004. Adjustment of Airborne Laser Altimetry Strips. *The International Archives of the Photogrammetry, Remote Sensing and Spatial Information Sciences*, 35 (B3), pp. 285-289.

Glennie, C.L., 2007. Rigorous 3D error analysis of kinematic scanning Lidar systems. *Journal of Applied Geodesy*, 1, pp. 147-157.

Habib, A., K. Bang, A. P. Kersting, and D. C. Lee, 2009a. Error Budget of LiDAR Systems and Quality Control of the Derived Data. *Photogrammetric Engineering and Remote Sensing*, 75(9), pp. 1093–1108.

Habib, A., A. P. Kersting, K. I. Bang, and M. Al-Durgham, 2009b. A Strip Adjustment Procedure to Mitigate the Impact of Inaccurate Mounting Parameters in Parallel LiDAR Strips. *The Photogrammetric Record*, 24(126), pp. 171-195.

Habib, A., A. P. Kersting, K. Bang, and D. C. Lee, 2010. Alternative Methodologies for the Internal Quality Control of Parallel LiDAR Strips. *IEEE Transactions on Geoscience and Remote Sensing,* 48(1), pp. 221-236.

Huising, E. J., and L. M. G. Pereira, 1998. Errors and Accuracy Estimates of Laser Data Acquired by various Laser Scanning Systems for Topographic Applications. *ISPRS Journal of Photogrammetry and Remote Sensing*, 53(5): 245-261.

Kager, H., 2004. Discrepancies Between Overlapping Laser Scanning Strips- Simultaneous Fitting of Aerial Laser Scanner Strips. *Proceedings of the International Society for Photogrammetry and Remote Sensing XXth Congress*, Istanbul, 34(B/1): 555 - 560.

Kilian, J., N. Haala, and M. Englich, 1996. Capture and evaluation of airborne laser scanner data. *International Archives of Photogrammetry and Remote Sensing*, 31(B3):383–388.

Maas H. G., 2002. Method for measuring height and planimetry discrepancies in airborne laserscanner data. *Photogrammetric Engineering and Remote Sensing*, 68(9): 933–940.

Morin, K.W., 2002. *Calibration of Airborne Laser Scanners*. M.S. thesis, University of Calgary, Department of Geomatics Engineering. 125 pages.

Pfeifer, N., S. O. Elberink, and S. Filin, 2005. Automatic Tie Elements Detection for Laser Scanner Strip Adjustment. *International Archives of Photogrammetry and Remote Sensing*, 36(3/W3): 1682-1750.

Schenk, T., 2001. Modeling and Analyzing Systematic Errors in Airborne Laser Scanners, *Technical Report in Photogrammetry* No. 19, Ohio Sate University. 42 pages.

Shin, S., Habib, A., Ghanma, M., Kim, C., and Kim, E., 2007. Algorithms for Multi-Sensor and Multi-Primitive Photogrammetric Triangulation. *ETRI Journal*, 29(4), pp. 411-420.

Skaloud, J. and D. Lichti, 2006. Rigorous Approach to Bore-Sight Self-Calibration in Airborne Laser Scanning. *ISPRS Journal of Photogrammetry and Remote Sensing*, 61: 47–59.

Toth, C. K., 2002. Calibrating Airborne Lidar Systems. http://www.isprs.org/commission2/proceedings02/paper/084_100.pdf [Accessed: 15th November 2007].

Vaughn, C. R., J. L. Bufton, W. B. Krabill, and D. L. Rabine, 1996. Georeferencing of Airborne Laser Altimeter Measurements. *International Journal of Remote Sensing*, 17(11): 2185-2200.